www.ietdl.org

Published in IET Networks
Received on 11th January 2012
Revised on 28th May 2012
doi: 10.1049/iet-net.2011.0028

ISSN 2047-4954

Optimal and sub-optimal resource allocation in multi-hop cognitive radio networks with primary user outage constraint

M.V. Nguyen[1] *T.Q. Duong*[2] *C.S. Hong*[1] *S. Lee*[1] *Y. Zhang*[3,4]

[1]*Department of Computer Engineering, Kyung Hee University, 446-701, Republic of Korea*
[2]*Blekinge Institute of Technology, School of Computing, SE-37179 Karlskrona, Sweden*
[3]*Department of Informatics, University of Oslo, Oslo, Norway*
[4]*Simula Research Laboratory, Martin Linges v17, Fornebu, P.O. Box 134, 1325 Lysaker, Norway*
E-mail: nvmui@khu.ac.kr

Abstract: In this study, the authors propose a cross-layer optimisation framework for cognitive radio networks (CRNs) by jointly taking into account the physical layer and transport layer. In particular, they focus on joint rate and power control for a multi-hop CRN to maximise the network utility without affecting the performance of primary users (PUs). The formulation is shown to be a non-linear non-convex optimisation problem. To solve the problem, the authors first use a successive convex approximation method, which has been proved to converge to the global optimum. Then, the authors propose a novel heuristic method to develop a practical sub-optimal distributed algorithm without explicit message passing. The authors have proved that the proposed distributed algorithm is able to converge to the unique fixed point near the global optimum. Finally, the illustrative results indicate that the proposed sub-optimal algorithm outperforms the high-signal-to-interference-ratio-based algorithm and closely approaches the global optimum.

1 Introduction

Cognitive radio networks (CRNs) have recently gained substantial attention for improving the spectrum efficiency and systems co-existence in wireless communications and networks. With the explosive traffic increase and highly dynamic wireless channel, it is very challenging to achieve the bandwidth and network efficiency in CRNs. Efficient resource management is one of the key components in CRNs to address this challenge. It has been accepted in the community that the throughput in a multi-hop CRN is tightly coupled with the lower-layer behaviours [1]. Network utility is dependent on congestion control algorithms at the transport layer, routing protocols at the network layer and channel assignments at the link layer, as well as power allocation at the physical layer. As a consequence, the overall performance of a multi-hop CRN calls for a cross-layer design and optimisation approach. The major motivation in this paper is to provide high throughput and resource usage for secondary users (SUs) via a cross-layer methodology without degrading the performance of primary users (PUs).

In the literature, there are several studies on resource allocation design under spectrum overlay paradigm in which spectrum sensing [2] needs performing at each SU before channel access in order to avoid possible collisions with PUs (e.g. [3–6]). In fact, spectrum sensing-based resource allocation poses significant challenges as well as limitations. There will be no transmissions from SUs, while a PU system operating under full load can tolerate more interference. In spectrum underlay systems, SUs are allowed to simultaneously transmit along with PUs over the same licensed bands as long as the total interference caused by them at the PU receiver (PU-Rx) is acceptable. To keep track of interference aggregated at PU-receivers, CRNs require a central controller to effectively cooperate with PUs [7, 8]. These works utilised signal-to-interference-ratio (SIR) at a receiving node as the quality-of-service (QoS) constraint for both SUs and PUs in a joint rate and power control (JRPC) optimisation problem. Such a hard constraint may be inappropriate for flexible QoS adaptation.

Some works (e.g. [3, 7–10]) have focused on the optimal resource allocation to maximise the throughput of SUs in single-hop CRNs with infrastructure. In this paper, we aim at JRPC problem in the more general setting of spectrum sharing-based multi-hop networks. Shiang and van der Schaar [4] proposed a distributed resource management solution using adaptive fictitious play approach to significantly improve the end-to-end delay for delay-sensitive applications. The study in [11] has proposed a game-theoretical approach to solve the JRPC issue in a code division multiple access (CDMA) cell-based CRN, where players compete selfishly. The optimal usage of network resources with respect to bandwidth and energy can be achieved, whereas the significant QoS metric fairness cannot be guaranteed. The recent work in [12] has developed an SIR approximation approach to solve the JRPC issue. Fairness has been considered under high-SIR regime because of fading margins. By utilising 1-bit outage feedback in the absence of PU cooperation, Huang *et al.* [13] have formulated the spectrum utilisation as a convex optimisation problem and proposed a distributed power control algorithm to maximise the total utility in the high-SIR regime. The aforementioned studies have assumed that each pair of secondary links cannot communicate with each other, and hence ignored the SUs' self-interference.

In this paper, we focus on the JRPC in CRNs with primary link protection. The main objective is to maximise the aggregate throughput of all SUs without affecting the performance of PUs in a distributed manner, that is, neither cooperation with the PUs nor requirement of central controllers. Therefore SUs need to flexibly perform adaptation according to the time-varying nature of fading environments in order to keep PUs' QoS stable during their update interval. To cope with the severe fading effect, the outage probability [14, 15], which is defined as the fraction of time a pair of transmitter/receiver experiences an outage over fading blocks, is chosen to best evaluate PU's quality of spectrum-sharing services. Consequently, the optimal values are not necessary to be updated whenever the fading channel changes their states. We propose a cross-layer optimisation framework by investigating the JRPC problem via network utility maximisation [16]. Our proposed model allows the SUs to periodically perform their rate and power updates without depending on dynamic fading channel. Our major contributions to address resource allocation in CRNs, which also demonstrate the difference from the existing studies are summarised as follows:

- A cross-layer framework is developed in multi-hop CRNs with the outage constraint as a non-linear non-convex optimisation problem. By using the successive convex approximation method, the resultant solution has been proved to converge to the global optimum.
- We propose a novel heuristic method to develop a practical sub-optimal distributed algorithm without explicit message passing. We have proved that the distributed algorithm is able to converge to the point near the global optimum.
- Another solution is also derived through high-SIR approximation to show the inherent trade-off between throughput and convergence rate for the proposed algorithms.

The rest of paper is organised as follows. Section 2 presents the system model and problem formulation. Section 3 introduces the optimally distributed algorithm based on the successive convex approximations method. In Section 4, we develop a new and practical rate and power control algorithm in order to obtain fast convergence speed with no explicit message passing. High-SIR approximation problem is derived in Section 5. Numerical results and conclusions are illustrated in Sections 6 and 7.

2 System model and problem formulation

We focus on CDMA-based multi-hop CRNs in which N SUs simultaneously access the same frequency band W licensed to a pair of PUs in a non-intrusive manner. We also consider the fluid-flow model at the transport layer, where a set of logical links $\mathcal{L} = \{1, \ldots, L\}$ is shared by a set of sources $\mathcal{S} = \{1, \ldots, S\}$. Each source s traverses multiple hops to reach its destination through a fixed set of links $L(s)$, the so-called route. The source s regulates its rate x_s according to congestion levels within the network. This is typically achieved by using a utility $U_s(x_s)$, which is assumed twice continuously differentiable, non-decreasing and strictly concave.

2.1 Fading model and capacity conservation

In the physical layer, all SUs can perform simultaneous two-way information transfer over a common radio channel known as division-free duplex [17]. Each transceiver is equipped with an omnidirectional dual-antenna, an adaptive RF isolator and an echo canceller in order to significantly mitigate the self-interference for full-duplex transmission. Let η_l denote the thermal noise power under bandwidth W at each receiver of link l. The instantaneous SIR at receiver of link l is defined as

$$\mathrm{SIR}_l(\boldsymbol{P}) = \frac{S_{ll}P_l}{\eta_l + \sum_{k\neq l} S_{lk}P_k + G_{l0}F_{l0}P_0} \quad (1)$$

where $\boldsymbol{P} = [P_1, \ldots, P_L]$ is a transmit power vector of secondary links and P_0 is the transmit power of primary link. $S_{lk} = G_{lk}F_{lk}$, where G_{lk} and F_{lk} represent the large-scale path gain and small-scale Rayleigh channel fading between the transmitter of link k and the receiver of link l, respectively. In this paper, we assume that $G_{lk} = d_{lk}^{-n}$ only depend on physical link distance d_{lk} with path loss exponent n while F_{lk} are assumed to be independent and identically distributed random variables (RVs). For notational simplicity, we define $\mathcal{L}' = \{0, 1, \ldots, L\}$ as the set of all secondary and the primary links and the index $l = 0$ represents the primary link.

We further assume that the channel is block fading, that is, F_{lk} are constant within the duration of power update interval, but vary independently over time scale of interests. As a result, the instantaneous Shannon capacity of link l is given by

$$C_l(\boldsymbol{P}) = W\log(1 + K\,\mathrm{SIR}_l(\boldsymbol{P})) \quad (2)$$

which keeps unchanged during a power adaption interval. Here, $K = -\phi_1/\log(\phi_2\mathrm{BER})$; ϕ_1 and ϕ_2 are constants depending on the modulation and coding scheme and bit error rate (BER) [18]. Note that log() represents the natural logarithm. Without loss of generality, we assume that K and W are unit henceforth. Capacity constraint for each link l is

$$\sum_{s\in S(l)} x_s \le C_l(\boldsymbol{P}), \quad \forall l \in \mathcal{L} \quad (3)$$

where $S(l) = \{s: l \in L(s)\}$ is the set of sources using link l.

2.2 Primary link protection

Owing to the coexistence of both PUs and SUs on the same frequency band, the total interference caused by SUs can make the primary link outage. To guarantee the PU's QoS, this interference at PU-Rx should be maintained at an acceptable level. In a Rayleigh-fading environment, SUs need to perform power adaptation according to the time-varying nature of fading environments in order to satisfy PU's QoS requirement during their power adaption interval.

IET Networks, 2012, Vol. 1, Iss. 2, pp. 47–57
doi: 10.1049/iet-net.2011.0028

Instantaneous $\mathrm{SIR}_0(\boldsymbol{P})$ at PU-Rx is defined as

$$\mathrm{SIR}_0(\boldsymbol{P}) = \frac{G_{00}F_{00}P_0}{\eta_0 + \sum_{k\in\mathcal{L}} G_{0k}F_{0k}P_k} \tag{4}$$

In the absence of SUs, a fast Rayleigh fading may make PU-Rx unable to decode the signal from PU-Tx. In such a case, the outage probability of primary link should be taken into account to protect the primary system. To allow SU's channel access while maintaining its QoS, PU-Rx requires its outage probability to stay below a certain threshold ζ_{th}

$$\Pr[\mathrm{SIR}_0(\boldsymbol{P}) \le \gamma_{\mathrm{th}}] \le \zeta_{\mathrm{th}} \tag{5}$$

where γ_{th} is the SIR threshold at PU-Rx.

2.3 Problem formulation

Our JRPC objective is to maximise the overall utility subject to capacity constraints (3) and the PU outage requirement (5) as follows

$$(\boldsymbol{P}1) \quad \max_{\boldsymbol{x}\in\mathcal{X},\boldsymbol{P}\in\mathcal{P}} \sum_{s\in\mathcal{S}} U_s(x_s) \quad \text{s.t.} \quad (3), (5) \tag{6}$$

where $\mathcal{X} = \{x_s, s\in\mathcal{S} | x_s^{\min} \le x_s \le x_s^{\max}\}$ and $\mathcal{P} = \{P_l, l\in\mathcal{L} | P_l^{\min} \le P_l \le P_l^{\max}\}$ indicate QoS constraints for each source and the hardware restrictions for each node. The optimisation problem ($\boldsymbol{P}1$) poses that the capacity of each link is a non-linear and neither convex nor concave function with respect to the optimisation variable, that is, the transmit power vector $\boldsymbol{P}$. The capacity constraint on each link becomes non-linear and non-convex on ($\boldsymbol{x}$, $\boldsymbol{P}$) which makes $\boldsymbol{P}1$ be a non-linear non-convex optimisation problem, and is generally not trivial to solve.

3 Jointly optimal rate and power control

3.1 Approximated convex problem

Let us rewrite the Shannon capacity $C_l(\boldsymbol{P})$, $\forall l \in \mathcal{L}$ given in (2) as follows

$$C_l(\boldsymbol{P}) = \log\left(\eta_l + \sum_{l\in\mathcal{L}'} S_{ll}P_l\right) - \log\left(\eta_l + \sum_{k\in\mathcal{L}'\setminus\{l\}} S_{lk}P_k\right) \tag{7}$$

Theorem 1: For a given power vector $\boldsymbol{P}$, there exists a weight vector $\boldsymbol{w}^l = (w_0^l, w_1^l, \ldots, w_{L+1}^l) \pm 0$, $\forall l\in\mathcal{L}$ satisfying

$$\begin{aligned} w_{L+1}^l &= \frac{\eta_l}{\eta_l + \sum_{k\in\mathcal{L}'} S_{lk}P_k}; \\ w_k^l &= \frac{S_{lk}P_k}{\eta_l + \sum_{k\in\mathcal{L}'} S_{lk}P_k}, \quad \forall k\in\mathcal{L}' \end{aligned} \tag{8}$$

such that $\tilde{C}_l(\boldsymbol{P}, \boldsymbol{w}^l) = C_l(\boldsymbol{P})$, where

$$\tilde{C}_l(\boldsymbol{P}, \boldsymbol{w}^l) = \sum_{k=0}^{L} w_k^l \log\left(\frac{S_{kk}P_k}{w_k^l}\right) + w_{L+1}^l \log\left(\frac{\eta_l}{w_{L+1}^l}\right) - \log\left(\eta_l + \sum_{k\in\mathcal{L}'\setminus\{l\}} S_{lk}P_k\right) \tag{9}$$

Proof: See Appendix 1. □

Now, we consider the constraint on PU's outage probability in (6). Based on the exponential distribution of RVs F_{0l}, $\forall l\in\mathcal{L}'$ in (5), the outage probability at PU-Rx for a transmit power vector $\boldsymbol{P}$ is given in [15]

$$\Pr[\mathrm{SIR}_0(\boldsymbol{P}) \le \gamma_{\mathrm{th}}] = 1 - (1-\zeta_0)\prod_{l=1}^{L}\left(1 + \gamma_{\mathrm{th}}\frac{G_{0l}P_l}{G_{00}P_0}\right)^{-1} \tag{10}$$

where $\zeta_0 = 1 - \exp(-\eta_0\gamma_{\mathrm{th}}/G_{00}P_0)$ is the primary outage probability because of Rayleigh fading in the absence of SUs. In this regard, we yield the lower bound on a posynomial function in $\boldsymbol{P}$

$$\prod_{l=1}^{L}(1 + \rho_l P_l) \le \mu \tag{11}$$

where $\mu = (1-\zeta_0)/(1-\zeta_{\mathrm{th}})$ is the relative margin of PU-Rx to accommodate the SU transmission and is greater than one since $\zeta_{\mathrm{th}} \ge \zeta_0$. $\rho_l = (G_{0l}\gamma_{\mathrm{th}}/G_{00}P_0)$ represents the interference effect per power unit caused by SU transmitter at link l to PU-Rx [13]. Without loss of optimality, the constraint set in (6) can be rewritten using the log change of power variables, that is, $\hat{\boldsymbol{P}} = \log\boldsymbol{P}$, in its corresponding domain as follows

$$(\boldsymbol{P}2) \quad \max_{\boldsymbol{x}\in\mathcal{X},\hat{\boldsymbol{P}}\in\hat{\mathcal{P}}} \sum_{s\in\mathcal{S}} U_s(x_s) \tag{12}$$

$$\text{s.t.} \begin{cases} \sum_{s\in S(l)} x_s \le \tilde{C}_l(\hat{\boldsymbol{P}}, \boldsymbol{w}^l), & \forall l\in\mathcal{L} \\ \sum_{l=1}^{L} \log(1 + \rho_l e^{\hat{P}_l}) \le \log\mu \end{cases}$$

The weight vector $\boldsymbol{w}^l$ is given by Theorem 1, $\hat{\mathcal{P}} = \{\hat{P}_l, l\in\mathcal{L} | \log P_l^{\min} \le \hat{P}_l \le \log P_l^{\max}\}$, and

$$\tilde{C}_l(\hat{\boldsymbol{P}}, \boldsymbol{w}^l) = \sum_{k=0}^{L} w_k^l \log\left(\frac{S_{lk}e^{\hat{P}_k}}{w_k^l}\right) + w_{L+1}^l \log\left(\frac{\eta_l}{w_{L+1}^l}\right) - \log\left(\eta_l + \sum_{k\in\mathcal{L}'\setminus\{l\}} S_{lk}e^{\hat{P}_k}\right) \tag{13}$$

Theorem 2: $\boldsymbol{P}2$ is a separable approximated convex optimisation problem in new variable space ($\boldsymbol{x}$, $\hat{\boldsymbol{P}}$) if we fix $\boldsymbol{w}^l$, $\forall l\in\mathcal{L}$ with any values of $\hat{\boldsymbol{P}} \in \hat{\mathcal{P}}$.

Proof: See Appendix 2. □

3.2 Dual decomposition

$\boldsymbol{P}2$ can be relaxed by transferring the constraints to the objective function in the form of a weighted sum. Its dual problem is then expressed as an unconstraint max–min problem

$$\min_{\lambda,\nu}\max_{x,\hat{\boldsymbol{P}}} L(\boldsymbol{x}, \hat{\boldsymbol{P}}, \boldsymbol{\lambda}, \nu) = \sum_{s\in\mathcal{S}} U_s(x_s) - \sum_{s\in\mathcal{S}}\sum_{l\in L(s)} \lambda_l x_s + \sum_{l\in\mathcal{L}} \lambda_l \tilde{C}_l(\hat{\boldsymbol{P}}, \boldsymbol{w}^l) - \nu\left(\sum_{l=1}^{L} \log(1+\rho_l \mathrm{e}^{\hat{P}_l}) - \log\mu\right) \quad (14)$$

where $L(\boldsymbol{x}, \hat{\boldsymbol{P}}, \boldsymbol{\lambda}, \nu) = L_x(\boldsymbol{x}, \boldsymbol{\lambda}) + L_{\hat{P}}(\hat{\boldsymbol{P}}, \boldsymbol{\lambda}, \nu)$ is Lagrangian and $\lambda = [\lambda_1, \ldots, \lambda_L]$ and ν are the Lagrange non-negative multipliers. λ and ν are interpreted as congestion prices and primary outage price, respectively. Theorem 2 indicates that the maximisation (14) can be decomposed into two subproblems with respect to primal variables $\boldsymbol{x}$ and $\hat{\boldsymbol{P}}$

$$\max_{\boldsymbol{x}}\left\{L_x(x, \lambda) = \sum_{s\in\mathcal{S}} U_s(x_s) - \sum_{s\in\mathcal{S}}\sum_{l\in L(s)} \lambda_l x_s\right\} \quad (15)$$

$$\max_{\hat{\boldsymbol{P}}}\left\{L_{\hat{\boldsymbol{P}}}(\hat{\boldsymbol{P}}, \boldsymbol{\lambda}, \nu) = \sum_{l\in\mathcal{L}} \lambda_l \tilde{C}_l(\hat{\boldsymbol{P}}, \boldsymbol{w}^l) - \nu \sum_{l\in\mathcal{L}} \log(1+\rho_l \mathrm{e}^{\hat{P}_l}) + \nu \log\mu\right\} \quad (16)$$

The first subproblem (15) is the rate control problem that is implicitly solved by the congestion control mechanism in wired networks [19] where the data rate of each source s is adjusted via the aggregate price $\lambda_s \doteq \sum_{l\in L(s)} \lambda_l$ for all links in path s. The second subproblem (16) is the power allocation problem in which the interference impact and energy efficiency are taken into account. Although it cannot be decomposed into local problems for each link, it is differentiable for all $\boldsymbol{P}$. This allows us to solve the power allocation problem by using projected gradient-ascent method in a distributed manner using message passing.

Since $\boldsymbol{P}2$ is a convex optimisation problem [Theorem 2], there exists a feasible point satisfying the Slater's constraint qualification [20] in its domain. From the strong duality theorem [21], there is no duality gap. Hence, the optimal solution can be obtained by solving the dual problem (14) via the following iterative optimiser.

3.2.1 Source and link optimiser (SLO):

At each time slot t, sources and links simultaneously perform their updates until convergence.

Congestion Control: The source rate updates

$$x_s^{(t+1)}(\lambda_s) = [U'^{-1}_s(\lambda_s^{(t)})]^{\mathcal{X}_s} \quad (17)$$

where $U'^{-1}_s(.)$ is the inverse of the first derivative of utility.

Power Control: The link power updates

$$P_l^{(t+1)} = \left[P_l^{(t)} + \kappa_t\left(\frac{\lambda_l^{(t)} w_l^l}{P_l^{(t)}} - \sum_{k\neq l} m_k^{(t)} S_{kl} - \nu^{(t)} \frac{\rho_l}{1+\rho_l P_l^{(t)}}\right)\right]^{\mathcal{P}_l} \quad (18)$$

where $m_k^{(t)} = (\lambda_k^{(t)} \mathrm{SIR}_k^{(t)}/S_{kk} P_k^{(t)})$.

Congestion price updates:

$$\lambda_l^{(t+1)} = \left[\lambda_l^{(t)} + \kappa_t\left(\sum_{s\in S(l)} x_s^{(t)} - \tilde{C}_l(\boldsymbol{P}^{(t)}, \boldsymbol{w}^l)\right)\right]^{\boldsymbol{R}_+} \quad (19)$$

PU outage price updates:

$$\nu^{(t+1)} = \left[\nu^{(t)} + \kappa_t\left(\sum_{l}^{L} \log(1+\rho_l P_l^{(t)}) - \log\mu\right)\right]^{\boldsymbol{R}_+} \quad (20)$$

Note that $[x]^{\mathcal{A}}$ represents the projection of x onto the feasible set $\mathcal{A}$ and κ_t is the positive scalar diminishing step-size.

We also note that SLO is implemented in a distributed manner:

- Source algorithm can preserve the existing TCP congestion mechanism in which source s adjusts its rate using (17) via the aggregate price λ_s for all links in the path s.
- From link algorithm, the SU-Rx of link k locally measures $\mathrm{SIR}_k(\boldsymbol{P})$ and broadcasts its control message RxCtrlMsg containing $m_k^{(t)}$. SU-Tx of link k receives RxCtrlMsg with $m_j^{(t)}$ and TxCtrlMsg with $P_j^{(t)}$ from the jth SU-Tx, estimates S_{jk} through training sequence, and updates power using (18) through congestion price (19), PU outage price (20) and w_l^l. Then SU-Tx broadcasts TxCtrlMsg with $P_k^{(t)}$.

Proposition 1: Given (λ, ν), source rate updates (17) and link power updates (18) solve the subproblems (15) and (16), respectively.

Proof: See Appendix 3. □

In the dual problem (14), the objective function is differential for all λ and ν. Therefore we can also apply the projected gradient-descent method [21] to solve the minimisation problem (15) via link congestion price updates (19) and PU outage price updates (20). From Propositions 1 and 2, we conclude that SLO solves $\boldsymbol{P}2$. For any initial values of primal and dual variables and the step-size satisfying

$$\kappa_t \geq 0, \quad \lim_{t\to\infty} \kappa_t = 0, \quad \sum_{t=0}^{\infty} (\kappa_t) = \infty, \quad \sum_{t=0}^{\infty} (\kappa_t)^2 < \infty \quad (21)$$

SLO always converges to a unique point [21]. Since $\boldsymbol{P}2$ is an approximated convex problem of $\boldsymbol{P}1$ [Theorem 2], any optimal point achieved by SLO is the local optimum of $\boldsymbol{P}1$.

3.3 Global optimality via condensation method

We consider the vector $\boldsymbol{w}^l (l \in \mathcal{L})$ in problem (12). It is obtained from any initial power vector $\boldsymbol{P} (P \in \mathcal{P})$ to keep

doi: 10.1049/iet-net.2011.0028

$\tilde{C}_l(\boldsymbol{P}, \boldsymbol{w}^l)$ in solving $\boldsymbol{P}2$. However, link capacity $C_l(\boldsymbol{P})$ in $\boldsymbol{P}1$ is continuously adjusted towards optimality with power control policy. Therefore the optimal solution achieved from SLO for $\boldsymbol{P}2$ may violate some certain constraints in $\boldsymbol{P}1$. In this regard, the solution can be further improved towards the global optimum by solving a sequence of approximated convex problems formulated from $\boldsymbol{P}2$ via the following Op-JRPC Algorithm.

Algorithm 1: Optimal JRPC Algorithm (Op-JRPC)

1. Initialise $\boldsymbol{x}^{(0)} \in \mathcal{X}$, $\boldsymbol{P}^{(0)} \in \mathcal{P}$, $(\lambda^{(0)}, \nu^{(0)}) \geq 0$, and counter $\tau = 1$.
2. Repeat
3. Compute $\boldsymbol{w}^{l(\tau)}$ based on $\boldsymbol{P}^{*(\tau-1)}$.
4. Form the τ^{th} approximated convex problem $\boldsymbol{P}2$.
5. Solve the τ^{th} approximated problem via SLO to obtain the local optimum $(\boldsymbol{x}^{*(\tau)}, \boldsymbol{P}^{*(\tau)})$.
6. Increment τ.
7. Until $\|\boldsymbol{P}^{*(\tau)} - \boldsymbol{P}^{*(\tau-1)}\| \leq \varepsilon$, where ε is the error tolerance.

In the τth iteration, the most violated constraint is condensed at the optimum $(\boldsymbol{x}^{*(\tau)}, \boldsymbol{P}^{*(\tau)})$ by SLO. This result is used to form the $(\tau+1)$th successive convex problem $\boldsymbol{P}2$ by updating the weight vector $\boldsymbol{w}^{l(\tau+1)}(\boldsymbol{P}^{*(\tau)})$. Through this procedure, the global optimum will be achieved when all constraints in the original problem $\boldsymbol{P}1$ are satisfied according to the certain convergence criteria, for example, $\|\boldsymbol{P}^{*(\tau)} - \boldsymbol{P}^{*(\tau-1)}\| \leq \varepsilon$.

Let $\tilde{g}_l(\boldsymbol{x}, \boldsymbol{P}) = \sum_{s\in S(l)} x_s/\tilde{C}_l(\boldsymbol{P}, \boldsymbol{w}^l)$ and $g_l(\boldsymbol{x}, \boldsymbol{P}) = \sum_{s\in S(l)} x_s/C_l(\boldsymbol{P})$, $\forall l \in \mathcal{L}$ denote the capacity constraint for the approximated problem $\boldsymbol{P}2$ and original problem $\boldsymbol{P}1$, respectively. The following three propositions will be the theoretical factual foundations for us to strongly conclude that Op-JRPC Algorithm converges to the global optimum.

Proposition 2: $\tilde{g}_l(\boldsymbol{x}, \boldsymbol{P}) \geq g_l(\boldsymbol{x}, \boldsymbol{P})$ for any $\boldsymbol{x} \in \mathcal{X}$, $\boldsymbol{P} \in \mathcal{P}$.

Proof: Since $\tilde{C}_l(\boldsymbol{P}, \boldsymbol{w}^l) \leq C_l(\boldsymbol{P})$, $\forall \boldsymbol{w}_l \pm 0$ and $\sum_i w_i^l = 1$ which derived from (42) in Appendix 1. □

Proposition 3: If $(\boldsymbol{x}^{*(\tau)}, \boldsymbol{P}^{*(\tau)}, \lambda^{*(\tau)}, \nu^{*(\tau)})$ is the optimal solution of Op-JRPC Algorithm, then

$$\tilde{g}_l(\boldsymbol{x}^{*(\tau)}, \boldsymbol{P}^{*(\tau)}) = g_l(\boldsymbol{x}^{*(\tau)}, \boldsymbol{P}^{*(\tau)}) \tag{22}$$

Proof: See Appendix 4. □

Proposition 4

$$\nabla \tilde{g}_l(\boldsymbol{x}^{*(\tau)}, \boldsymbol{P}^{*(\tau)}) = \nabla g_l(\boldsymbol{x}^{*(\tau)}, \boldsymbol{P}^{*(\tau)}) \tag{23}$$

Proof: It is easily obtained by taking the derivative on both sides of (23).

Theorem 3: For any initial source rate $\boldsymbol{x}^{(0)} \in \mathcal{X}$, link power $\boldsymbol{P}^{(0)} \in \mathcal{P}$ and shadow prices $(\lambda^{(0)}, \nu^{(0)}) \geq 0$, the sequence of primal-dual variables generated by Op-JRPC Algorithm converges to the global optimum of the original problem $\boldsymbol{P}1$.

Proof: See Appendix 5. □

4 Sub-optimal resource allocation solution

As explained, the objective function $\sum_{s\in\mathcal{S}} U_s(x_s)$ in the non-convex problem $\boldsymbol{P}1$ is the sum of concave functions (e.g. $U_s(x_s) = \log(x_s)$ [19]). It is separable in the optimisation variables $(\boldsymbol{x}, \boldsymbol{P})$. In addition, $\boldsymbol{x}$ and $\boldsymbol{P}$ can also be disjoined although they are coupled together in the constraints on the link capacity and primary outage probability of $\boldsymbol{P}1$. Hence, we can directly apply the dual decomposition technique into the original problem $\boldsymbol{P}1$'s Lagrangian function. Following the similar reasoning in Section 3, we can obtain the dual problem

$$\min_{\lambda,\nu} \max_{\boldsymbol{x},\boldsymbol{P}} \{L(\boldsymbol{x}, \boldsymbol{P}, \boldsymbol{\lambda}, \nu) = L_{\boldsymbol{x}}(\boldsymbol{x}, \boldsymbol{\lambda}) + L_{\boldsymbol{P}}(\boldsymbol{P}, \boldsymbol{\lambda}, \nu)\} \tag{24}$$

where

$$L_{\boldsymbol{x}}(\boldsymbol{x}, \boldsymbol{\lambda}) = \sum_{s\in\mathcal{S}} U_s(x_s) - \sum_{l\in\mathcal{L}} \lambda_l \sum_{s\in S(l)} x_s \tag{25}$$

$$L_{\boldsymbol{P}}(\boldsymbol{P}, \boldsymbol{\lambda}, \nu) = \sum_{l\in\mathcal{L}} \lambda_l C_l(\boldsymbol{P}) - \nu(\Pr[\text{SIR}_0(\boldsymbol{P}) \leq \gamma_{\text{th}}] - \zeta_{\text{th}}) \tag{26}$$

are the functionally partial Lagrangians.

The congestion control subproblem $\max_{\boldsymbol{x}\in\mathcal{X}} L_{\boldsymbol{x}}(\boldsymbol{x}, \boldsymbol{\lambda})$ is still the same as the one in Op-JRPC Algorithm. The power allocation subproblem $\max_{\boldsymbol{P}\in\mathcal{P}} L_{\boldsymbol{P}}(\boldsymbol{P}, \boldsymbol{\lambda}, \nu)$ is non-convex. Therefore we propose a new heuristic method to solve this second subproblem in which local measurements are used together with ACK/NACK feedback information on PU channel.

4.1 Estimation of PU outage probability

We first make the estimation of PU outage probability such that SUs can update PU outage price based on the feedback information on PU channel. Let N_T denote the number of outage events of the PU-Rx observed at secondary nodes during a power update interval $[(t-1)T, tT]$. Then, the noisy estimation of the PU outage probability, $\Pr[\gamma_0{}^k(\boldsymbol{P}^k) \leq \gamma_{\text{th}}{}^k]$, is [13]

$$\hat{\zeta}^{(t)} = \begin{cases} 1/T, & \text{if } N_T^{(t)} = 0 \\ N_T^{(t)}/T, & \text{otherwise} \end{cases} \tag{27}$$

Since $L(\boldsymbol{x}, \boldsymbol{P}, \lambda, \nu)$ is affine in λ and ν, its sub-gradients with respect to λ and ν are yielding

$$\partial L(\boldsymbol{x}, \boldsymbol{P}, \boldsymbol{\lambda}, \nu)/\partial\lambda_l = \sum_{s\in S(l)} x_s - C_l(\boldsymbol{P}) \tag{28}$$

$$\partial L(\boldsymbol{x}, \boldsymbol{P}, \boldsymbol{\lambda}, \nu)/\partial\nu = \zeta_{\text{th}} - \hat{\zeta} \tag{29}$$

The dual problem (24) can be solved using subgradient projection method [21], where the congestion prices $\lambda_l (l \in \mathcal{L})$ and PU outage price ν are adjusted in the descent direction of subgradients $\nabla_\lambda L(\boldsymbol{x}, \boldsymbol{P}, \lambda, \nu)$ and $\nabla_\nu L(\boldsymbol{x}, \boldsymbol{P}, \lambda, \nu)$.

4.2 Heuristic power allocation

By substituting the constraint on PU outage probability (11) into (26), we have the power allocation subproblem

$\max_{\boldsymbol{P}\in\mathcal{P}} L_{\boldsymbol{P}}(\boldsymbol{P}, \boldsymbol{\lambda}, \nu)$ as follows

$$\max_{\boldsymbol{P}\in\mathcal{P}} L_{\boldsymbol{P}}(\boldsymbol{P}, \boldsymbol{\lambda}, \nu) = \sum_{l\in\mathcal{L}} \lambda_l C_l(\boldsymbol{P}) - \nu\left(\sum_{l\in\mathcal{L}} \log(1+\rho_l P_l) - \log\mu\right) \quad (30)$$

The subproblem (30) shows that $L_{\boldsymbol{P}}(\boldsymbol{P}, \lambda, \nu)$ consists of two parts where the second item is separable and convex while the first item is contrary in $\boldsymbol{P}$. Therefore we take into account this inseparable non-convex portion, then equivalently transform the non-convex subproblem (30) into a convex optimisation problem. For the fixed ingress rate, the link powers $\boldsymbol{P}$ must be controlled such that the capacity on each link is equal to bandwidth demand, that is

$$\sum_{s\in S(l)} x_s = C_l(\boldsymbol{P}) = \log(1+\mathrm{SIR}_l(\boldsymbol{P})), \quad \forall l\in\mathcal{L} \quad (31)$$

Hence, the SIR requirement of each link at its assigned rate $\sum_{s\in S(l)} x_s$ is given by

$$\mathrm{SIR}_l(\boldsymbol{P}) \geq \exp\left(\sum_{s\in S(l)} x_s\right) - 1 \doteq \mathrm{SIR}_l^{\mathrm{th}}, \quad \forall l\in\mathcal{L} \quad (32)$$

Then, the power allocation subproblem (30) is equivalent to seeking a feasible power vector $\boldsymbol{P}$ to minimise the total interference impact on PU-Rx while meeting the incoming rate demand constraints (32)

$$\min_{\boldsymbol{P}\in\mathcal{P}} \quad h(\boldsymbol{P}) \doteq \nu\sum_{l=1}^{L} \log(1+\rho_l P_l) \quad (33)$$

$$\text{s.t.} \quad \mathrm{SIR}_l^{\mathrm{th}}/\mathrm{SIR}_l(\boldsymbol{P}) \leq 1, \quad \forall l\in\mathcal{L}$$

The set of constraints on SIR in the problem (33) can be rewritten as follows

$$P_l \geq \frac{\mathrm{SIR}_l^{\mathrm{th}}}{\Omega_l(\boldsymbol{P})} \doteq I_{-l}(\boldsymbol{P}), \quad \forall l\in\mathcal{L} \quad (34)$$

where

$$\Omega_l(\boldsymbol{P}) = \frac{G_{ll}}{\eta_l + \sum_{k\in\mathcal{L}'\backslash\{l\}} G_{lk}P_k} \quad (35)$$

and $I_{-l}(\boldsymbol{P})$ is the effective interference on the link l. We note that ν and x_s, respectively represent the primary outage status and the ingress rate before performing power update. Hence, in this regard, they are fixed. Since the objective of (33) is concave in $\boldsymbol{P}$, any feasible transmit power vector $\hat{\boldsymbol{P}}$ with minimum total power satisfied the set of constraints (34) is the optimal solution of (33). In this sense, we propose a power control algorithm to solve the problem (33) via the link power updates

$$P_l^{(t+1)} = \left[I_l(\boldsymbol{P}^{(t)}) - \nu^{(t)}\frac{\partial h(\boldsymbol{P}^{(t)})}{\partial P_l}P_l^{(t)}\right]^{\mathcal{P}_l}, \quad \forall l\in\mathcal{L} \quad (36)$$

4.3 Sub-optimal joint rate and power control algorithm

The optimal solution of $\boldsymbol{P}1$ can be found via the following iterative algorithm.

Algorithm 2: Sub-optimal JRPC algorithm (Sop-JRPC).

The primal and dual variables are updated iteratively until convergence.

Congestion control: The source rate updates as (17) in Op-JRPC.

$$x_s^{(t+1)}(\lambda_s) = [U'^{-1}_s(\lambda_s^{(t)})]^{\mathcal{X}_s}$$

Power control: The link power updates

$$P_l^{(t+1)} = \left[P_l^{(t)}\frac{\exp\left(\sum_{s\in S(l)} x_s^{(t)}\right) - 1}{\mathrm{SIR}_l(\boldsymbol{P}^{(t)})} - \nu^{(t)}\frac{\rho_l P_l^{(t)}}{1+\rho_l P_l^{(t)}}\right]^{\mathcal{P}_l} \quad (37)$$

Link Congestion price update:

$$\lambda_l^{(t+1)} = \left[\lambda_l^{(t)} + \kappa_t\left(\sum_{s\in S(l)} x_s^{(t)} - C_l(\boldsymbol{P}^{(t)})\right)\right]^{\boldsymbol{R}_+} \quad (38)$$

PU Outage Price update:

$$\nu^{(t+1)} = [\nu^{(t)} + \kappa_t(\hat{\zeta}^{(t)} - \zeta_{\mathrm{th}})]^{\boldsymbol{R}_+} \quad (39)$$

Proposition 5: Given $(\boldsymbol{x}, \nu)$, the iterative algorithm (37) always converges to a unique limit point $P_l^{(*)}$.

Proof: See Appendix 6. □

Theorem 4: For any initial source rate vector $\boldsymbol{x}^{(0)}\in\mathcal{X}$, link power vector $\boldsymbol{P}^{(0)}\in\mathcal{P}$, and shadow prices $(\lambda^{(0)}, \nu^{(0)}) \geq 0$, the limit point of the sequence of primal-dual variables generated by Sop-JRPC Algorithm is near the global optimum of the original optimisation problem $\boldsymbol{P}1$. □

Proof: See Appendix 7.

Sop-JRPC Algorithm can be implemented in a distributed manner.

- The congestion control mechanism is the same as the one in Op-JRPC algorithm.
- The power control requires only the link's local SIR measurement and the allocated ingress rate $\sum_{s\in S(l)} x_s^{(t)}$ without explicit message passing requirements. The update rule is that if the $\mathrm{SIR}_l(\boldsymbol{P}^{(t)})$ at time interval t is less than $\mathrm{SIR}_l^{\mathrm{th}}$, (i.e. $e^{\sum_{s\in S(l)} x_s^{(t)}} - 1$), then the link power needs to proportionally increase by a factor of $\mathrm{SIR}_l^{\mathrm{th}}/\mathrm{SIR}_l(\boldsymbol{P}^{(t)})$. This update rule satisfies the bandwidth demand of all links with the allocated ingress rate $\sum_{s\in S(l)} x_s^{(t)}$ while keeping the interference on PU-Rx below the tolerable limit via the PU outage price $\nu^{(t)}$.
- The congestion price update requires only the value of queue backlog on each link.
- The PU outage price update is based on the ACK/NACK feedback information of licensed channel overheard by secondary nodes.

IET Networks, 2012, Vol. 1, Iss. 2, pp. 47–57
doi: 10.1049/iet-net.2011.0028

5 Convex optimisation problem under high-SIR regime

In this section, we take into consideration the original problem $\boldsymbol{P}1$ under high-SIR regime which is extensively used in the literature (e.g. [12, 13] etc.) to approximate the interference-limited link capacity to be concave in the transmit power vector $\boldsymbol{P}$. We assume that there is no fading-margin at each link and $\text{SIR}_l(\boldsymbol{P})$, $l \in \mathcal{L}$ is much larger than 1. Then, Shannon capacity for each link can be approximated by

$$\begin{aligned}\tilde{C}_l(\boldsymbol{P}) &\simeq \log(\text{SIR}_l(\boldsymbol{P})) \\ &= \log(S_{ll}P_l) - \log\left(\eta_l + \sum_{k\in\mathcal{L}'\setminus\{l\}} S_{lk}P_k\right)\end{aligned} \quad (40)$$

After we change power variables and use the similar procedure in Section 2. The non-convex original problem $\boldsymbol{P}1$ becomes

$$(\boldsymbol{P}3) \quad \max_{\boldsymbol{x}\in\mathcal{X},\boldsymbol{P}\in\hat{\mathcal{P}}} \sum_{s\in\mathcal{S}} U_s(x_s) \quad (41)$$

$$\text{s.t.} \begin{cases} \sum_{s\in S(l)} x_s \le \hat{P}_l \log(S_{ll}) - \log\left(\eta_l + \sum_{k\in\mathcal{L}'\setminus\{l\}} S_{lk}\mathrm{e}^{\hat{P}_k}\right), \forall l \in \mathcal{L} \\ \sum_{l=1}^{L} \log(1+\rho_l \mathrm{e}^{\hat{P}_l}) \le \log \mu \end{cases}$$

It is clear that the approximated optimisation problem $\boldsymbol{P}3$ is convex. Therefore the optimal solution can be obtained by using standard convex optimisation techniques. This result is used to compare with the performance of our proposals, that is, Op-JRPC and Sop-JRPC in Section 6.

6 Numerical simulation and results

6.1 Simulation setting

We consider a simplified multi-hop CRN system which consists of 5 SU nodes, a pair of PUs, and four flows as shown in Fig. 1. We assume that TCP Vegas's utility function $U_s(x_s) = \log(x_s)$ is used to model the level of satisfaction of each source. Each secondary link with $P_l^{\min} = 26$ dBm can use the whole licensed bandwidth of 125 KHz. The minimum data rate for each elastic flow is 100 bps. The target BER $= 10^{-4}$ corresponding to MQAM modulation is the same for all secondary nodes with $K = -1.5/\log(5\text{BER})$ [18]. The large-scale fading channel gain only depends on physical link distance with path loss exponent $n = 4$. For PUs, outage probability is set to be $\zeta_{\text{th}} = 10\%$ for SIR threshold 0.41 dB at transmit power 20 dBm.

6.2 Relationships between rate control and power allocation via pricing

The numerical results are displayed in Figs. 2 and 3 to highlight the mutual relationships of rate control and power allocation via pricing. As depicted in Fig. 2 that there is a difference in power allocation strategies of Op-JRPC and Sop-JRPC. It can be observed from (18) in Op-JRPC algorithm that the transmission power per each link depends on not only its congestion level but also interference impact on the other links (including primary link). As a result, the congestion problem is simultaneously solved by both links (adjust their powers as shown in Fig. 2*a*) and sources (regulate their rates as shown in Fig. 3*a*) through the reflection of congestion prices subject to PU outage constraint. Hence, the variation between two consecutive adjustments is very small. On the contrary, we can see from (37) in Sop-JRPC algorithm that all links always conform their powers according to the changes of ingress rate demand (regulated by sources through congestion prices) subject to PU outage constraint. Consequently, the variations between two consecutive adjustments for both rate control and power allocation higher as shown in Figs. 1–3*b*.

6.3 Evolution of algorithms

In this experiment, we compare the evolution of the two proposed algorithms. The criterion used to evaluate the convergence speed is $\text{Max}\|\boldsymbol{P}^{*(t)} - \boldsymbol{P}^{*(t-1)}\| \le \varepsilon$, where ε is the error tolerance. Table 1 shows the impact of error tolerance on the convergence speed of algorithms (i.e. the minimum number of iteration to meet a certain convergence criterion).

More specifically, Fig. 4 shows that the trajectories of probabilities converge to the outage thresholds 10 and 15% for both algorithms. For the performance comparison

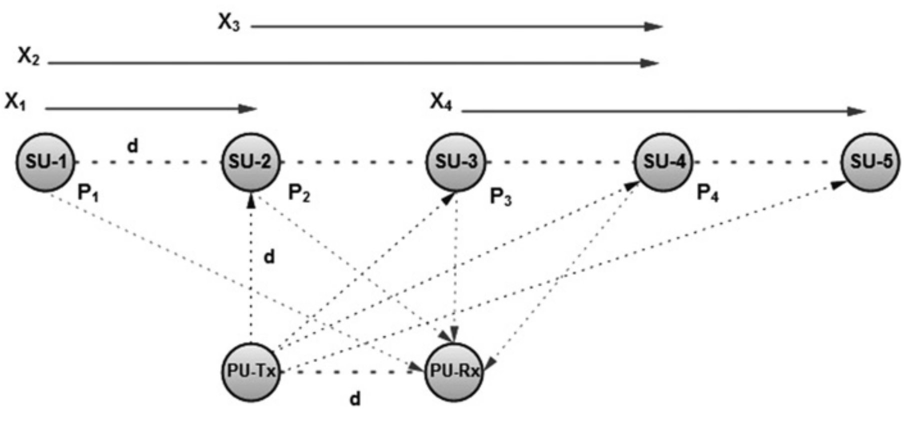

Fig. 1 *Physical and logical topologies for simulation*

doi: 10.1049/iet-net.2011.0028

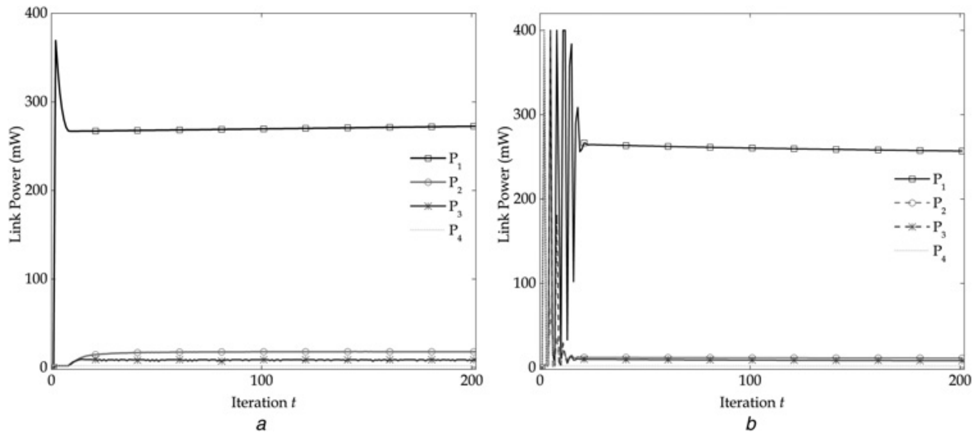

Fig. 2 *Convergence of link powers at the PU outage probability 10%*
a Op-JRPC
b Sop-JRPC

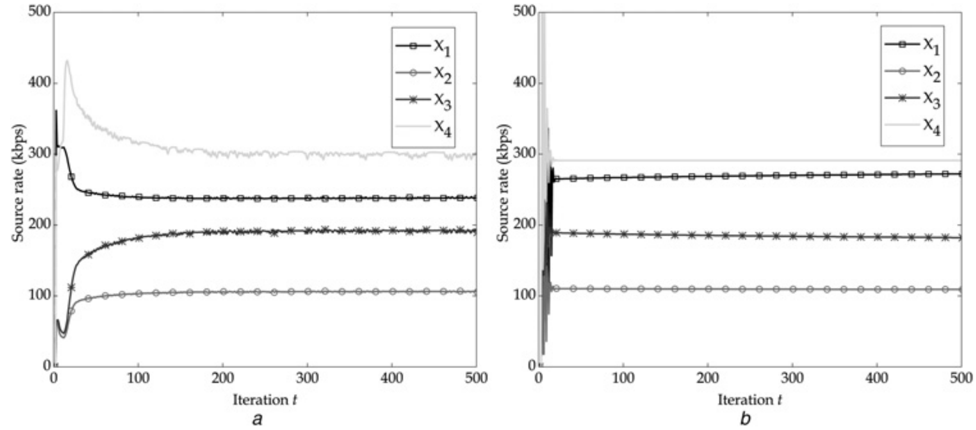

Fig. 3 *Trajectory of source rates at the PU outage probability 10%*
a Op-JRPC
b Sop-JRPC

Table 1 Convergence speed comparison of algorithms

ε	10^{-3}	10^{-4}	10^{-5}
Op-JRPC alg.	270	415	1199
high-SIR based alg.	65	320	361
Sop-JRPC alg.	21	26	45

between two algorithms, Sop-JRPC has a larger deviation during a transient time before converging to the fixed point. This deviation sometimes makes an excess of desired outage threshold. On the contrary, Op-JRPC algorithm always keeps the primary outage probabilities below 10 and 15%. However, it takes a longer time for Op-JRPC to reach the optimal point.

Fig. 5 also shows the trajectory of aggregated throughput. Although Sop-JRPC has a high variation during transient time, its convergence speed is much faster than those of Op-JRPC and high-SIR-based algorithm. We can realise that the aggregated throughput of both Op-JRPC and Sop-JRPC is almost indistinguishable and approaches to the global optimum at an error tolerance of 10^{-5}. Using high-SIR-based algorithm (e.g. [12, 13] etc.), we can achieve the sub-optimal throughput because the least average SIR required for accuracy is 10 and 15 dB with and without

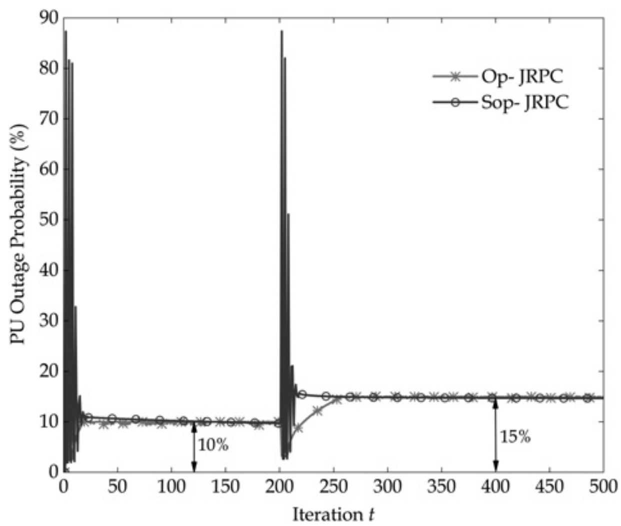

Fig. 4 *Convergence of PU outage probability with its thresholds 10 and 15%*

fading margins, respectively. Moreover, the high-SIR based JRPC algorithm exposes some drawbacks to implement in practice. Its performance will be fast-downgraded in low-SIR regions and message passing leads an un-scalability

doi: 10.1049/iet-net.2011.0028

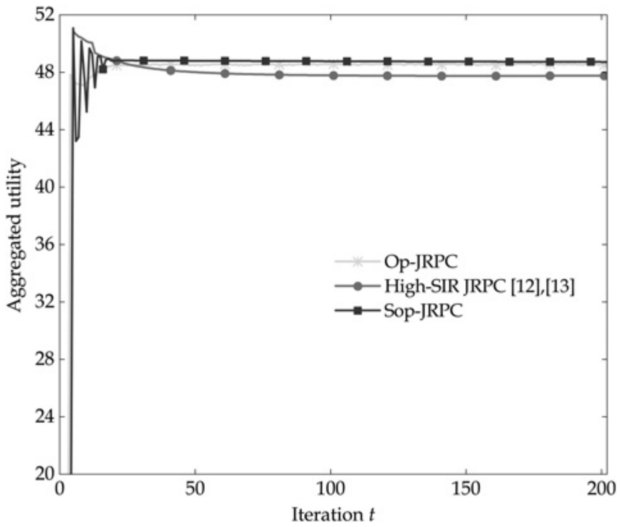

Fig. 5 *Comparison of aggregated utilities at the PU outage threshold $\zeta_{th} = 10\%$*

because of overhead. This observation verifies the feasibility of our novel heuristic-based algorithm Sop-JRPC.

6.4 Spectrum opportunity under spectrum sharing approach

In Fig. 6, we shows the achievable SIR of all links against PU outage thresholds. We assume that PU-Rx can successfully decode the received signal at SIR threshold 0.41 dB. With its fixed transmission power 20 dBm, primary link achieves the maximum SIR of 15 dB on the Rayleigh-fading channel. Hence, the primary SIR budget remains larger enough to tolerate more interference from SU's access. The primary outage probability requirement indicates how much the primary link's SIR budget should decrease in order to increase secondary system's throughput. Hence, the primary outage probability can be considered as a controllable valve via cross-layer rate and power design to decide the total throughput of secondary system at the risk of primary outage. In this regard, we confirm that secondary system can optimally exploit the primary spectrum if the PU outage probability still below acceptable threshold in an underlay manner.

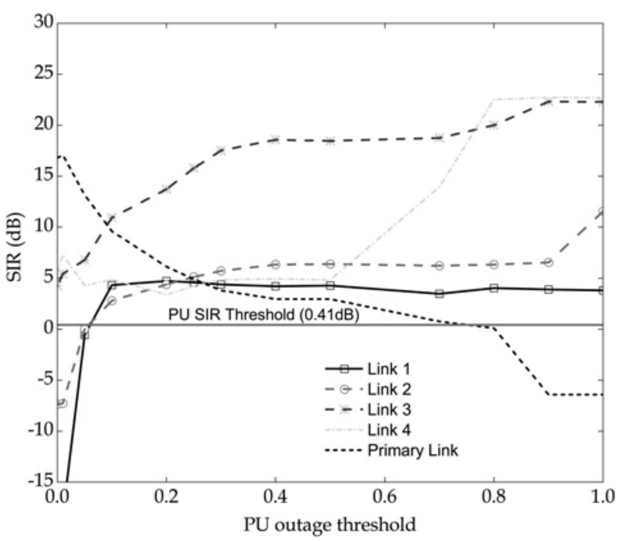

Fig. 6 *Effect of the primary QoS requirement on secondary link's SIR*

7 Conclusions

In this paper, we have formulated the optimisation problem for a cross-layer design of multi-hop CRNs under primary user outage constraint. As the link capacity constraints are neither convex nor concave, the formed optimisation problem is known to be $\mathcal{NP}$-hard [22]. Our first solution (i.e. Op-JRPC) is to solve a sequence of approximated convex problems so as to achieve the global optimal source rates and link powers for the original problem. However, its much slower convergence speed and explicit message passing requirements force us to propose a heuristic solution (i.e. Sop-JRPC), which circumvents the aforementioned drawbacks. Finally, we also revisited a high-SIR-based method to back-substitute the optimality of the proposed algorithms.

8 References

1 Shi, Y., Hou, T., Zhou, H., Midkiff, F.: 'Distributed cross-layer optimization for cognitive radio networks', *IEEE Trans. Veh. Technol.*, 2010, **59**, pp. 4058–4069
2 Chen, B.-Y., Chou, Y.-H., Chao, H.-C., Lo, C.-H.: 'Secure centralized spectrum sensing for cognitive radio networks', *Wirel. Netw.*, 2012 DOI:2012, 10.1007/s11276-012-0426-3
3 Urgaonkar, R., Neely, M.J.: 'Opportunistic scheduling with reliability guarantees in cognitive radio networks', *IEEE Trans. Mob. Comput.*, 2009, **8**, (6), pp. 766–777
4 Shiang, H.-P., van der Schaar, M.: 'Distributed resource management in multihop cognitive radio networks for delay-sensitive transmission', *IEEE Trans. Veh. Technol.*, 2009, **58**, (2), pp. 941–953
5 Carlos Cordeiro, D.B., Challapali, K., N, S.S.: 'IEEE 802.22: an introduction to the first wireless standard based on cognitive radios', *J. Commun.*, 2006, **1**, (1), pp. 38–47
6 Chen, Y.-S., Cho, C.-H., You, I., Chao, H.-C.: 'A cross-layer protocol of spectrum mobility and handover in cognitive lte networks', *Simul. Modelling Pract. Theory*, 2011, **19**, (8), pp. 1723–1744
7 Hoang, A.T., Liang, Y.-C., Islam, M.H.: 'Power control and channel allocation in cognitive radio networks with primary users' cooperation', *IEEE Trans. Mobile Comput.*, 2010, **9**, (3), pp. 348–360
8 Le, L.B., Hossain, E.: 'Resource allocation for spectrum underlay in cognitive radio networks', *IEEE Trans. Wirel. Commun.*, 2008, **7**, (12), pp. 5306–5315
9 Kang, X., Liang, Y.-C., Garg, H.K.: 'Fading cognitive multiple access channels: Outage capacity regions and optimal power allocation', *IEEE Trans. Wirel. Commun.*, 2010, **9**, (7), pp. 2382–2391
10 Kim, D., Le, L., Hossain, E.: 'Joint rate and power allocation for cognitive radios in dynamic spectrum access environment', *IEEE Trans. Wirel. Commun.*, 2008, **7**, (12), pp. 5517–5527
11 Zhou, P., Yuan, W., Liu, W., Cheng, W.: 'Joint power and rate control in cognitive radio networks: a game-theoretical approach'. Proc. IEEE ICC'08, Beijing, China, May 2008
12 Zhu, Y., Sun, Z., Wang, W., Peng, T., Wang, W.: 'Joint power and rate control considering fairness for cognitive radio network'. Proc. IEEE WCNC'09, Las Vegas, USA, March 2009
13 Huang, S., Liu, X., Ding, Z.: 'Distributed power control for cognitive user access based on primary link control feedback'. Proc. IEEE INFOCOM 2010, San Diego, CA, USA, March 2010, pp. 1–9
14 Caini, C., Immovilli, G., Merani, M.L.: 'Outage probability for cellular mobile radio systems: simplified analytical evaluation and simulation results', *IET Electron. Lett.*, 1992, **28**, (7), pp. 669–671
15 Kandukuri, S., Boyd, S.: 'Optimal power control in interference-limited fading wireless channels with outage-probability specifications', *IEEE Trans. Wireless Commun.*, 2002, **1**, (1), pp. 46–55
16 Kelly, F.P.: 'Charging and rate control for elastic traffic', *Eur. Trans. Tel.*, 1997, **8**, (1), pp. 33–37
17 Chen, S., Beach, M.A., McGeehan, J.P.: 'Division-free duplex for wireless applications', *IEEE Electron. Lett.*, 1998, **34**, (2), pp. 147–148
18 Goldsmith, A.: 'Wireless communications' (Cambridge University Press, Cambridge, UK, 2004)
19 Low, S.H., Peterson, L.L., Wang, L.: 'Understanding tcp vegas: a duality model', *J. ACM*, 2002, **49**, pp. 207–235

20 Bertsekas, D.: 'Convex analysis and optimization' (Athena Scientific, 2003)
21 Bertsekas, D.: 'Nonelinear programming' (Athena Scientific, 2003)
22 Kreinovich, V., Kearfott, R.: 'Beyond convex? global optimization is feasible only for convex objective functions: A theorem', *J. Global Optim.*, 2005, **33**, (0925-5001), pp. 617–624

9 Appendix 1: Proof of Theorem 1

The weighted arithmetic-geometric mean inequality states that $\Sigma_i w_i b_i \geq \prod_i b_i^{w_i}$ with $w_i \geq 0$, $b_i \geq 0\ \forall i$ and $\Sigma_i w_i = 1$. By letting $a_i = w_i b_i$, we have a similar inequality $\Sigma_i a_i \geq \prod_i (b_i/w_i)^{w_i}$ which holds with equality if and only if $w_i = a_i/\Sigma_i a_i$. Applying above inequality into $f_l(\boldsymbol{P}) \doteq \eta_l + \Sigma_{k\in\mathcal{L}'} S_{lk} P_k$ with $\boldsymbol{w}^l$, we have

$$\sum_{k\in\mathcal{L}'} S_{lk}P_k + \eta_l \geq \prod_{k=0}^{L}\left(\frac{S_{lk}P_k}{w_k^l}\right)^{w_k^l}\left(\frac{\eta_l}{w_{L+1}^l}\right)^{w_{L+1}^l} \tag{42}$$

By taking logarithm on both sides of (42), we achieve

$$\log\left(\eta_l + \sum_{k\in\mathcal{L}'} S_{lk}P_k\right) \geq \sum_{k=0}^{L} w_k^l \log\left(\frac{S_{lk}P_k}{w_k^l}\right) + w_{L+1}^l \log\left(\frac{\eta_l}{w_{L+1}^l}\right)$$

which leads $\tilde{C}_l(\boldsymbol{P}, \boldsymbol{w}^l) \leq C_l(\boldsymbol{P})$. The equality happens when $\boldsymbol{w}^l$ is given by (8).

10 Appendix 2: Proof of Theorem 2

We fix $\boldsymbol{w}^l (l \in \mathcal{L})$ with the value of $\hat{\boldsymbol{P}} \in \hat{\mathcal{P}}$. Hence, three problems in this theorem needs to be proved as follows: The first is the convexity in $\boldsymbol{P}2$ since $U_s(x_s)$ is strictly concave and the constraint set is convex (because log-sum-exp function is convex). The second is separability in $\boldsymbol{x}$ and $\hat{\boldsymbol{P}}$ because we can omit $\boldsymbol{x}$ or $\hat{\boldsymbol{P}}$ if we partially take the derivative of $\boldsymbol{P}2$ with respect to $\hat{\boldsymbol{P}}$ or $\boldsymbol{x}$. Finally, we can state that $\boldsymbol{P}2$ is an approximation of $\boldsymbol{P}1$ since $\tilde{C}_l(\hat{\boldsymbol{P}}, \boldsymbol{w}^l) \leq C_l(\hat{\boldsymbol{P}})$.

11 Appendix 3: Proof of Proposition 1

By taking the first-order derivative of $L_x(\boldsymbol{x}, \lambda)$ with respect to x_s, then we have (17) by letting the resulting quantity equal zero.

Similarly, we take first-order derivative of $L_{\hat{P}}(\hat{\boldsymbol{P}}, \boldsymbol{\lambda}, \nu)$ with respect to $\hat{P}_l$

$$\frac{\partial L_{\hat{P}}(\hat{\boldsymbol{P}}, \boldsymbol{\lambda}, \nu)}{\partial \hat{P}_l} = w_l^l \lambda_l - \sum_{k\neq l} \lambda_k \frac{S_{kl}\mathrm{e}^{\hat{P}_l}}{\sum_{j\neq k} S_{kj}\mathrm{e}^{\hat{P}_j} + S_{k0}\mathrm{e}^{\hat{P}_0} + \eta_0} - \nu\frac{\rho_l \mathrm{e}^{\hat{P}_l}}{1+\rho_l \mathrm{e}^{\hat{P}_l}} \tag{43}$$

Using the facts $\nabla_l L_P(\boldsymbol{P}, \boldsymbol{\lambda}, \nu) = (1/P_l)\nabla_l L_{\hat{P}}(\hat{\boldsymbol{P}}, \boldsymbol{\lambda}, \nu)$ and $P_l = \mathrm{e}^{\hat{P}_l}$, transforming (43) back to $\boldsymbol{P}$ space, and letting $m_k = (\lambda_k \mathrm{SIR}_k/S_{kk}P_k)$, we have

$$\frac{\partial L_P(\boldsymbol{P}, \boldsymbol{\lambda}, \nu)}{\partial P_l} = \frac{\lambda_l w_l^l}{P_l} - \sum_{k\neq l} m_k S_{kl} - \nu\frac{\rho_l}{1+\rho_l P_l} \tag{44}$$

Adopting the projected gradient-ascent method [21] with a step size $\kappa_t \geq 0$, we have the link power updates (18).

12 Appendix 4: Proof of Proposition 3

$\boldsymbol{w}^{l,(\tau)}$ is a function of the optimal point $(\boldsymbol{x}^{*(\tau-1)}, \boldsymbol{P}^{*(\tau-1)})$ achieved at the previous iteration. At $(\boldsymbol{x}^{*(\tau)}, \boldsymbol{P}^{*(\tau)})$, we have

$$\sum_{s\in S(l)} x_s^{*(\tau)} = \tilde{C}_l(\boldsymbol{P}^{*(\tau)}, \boldsymbol{w}^{l,(\tau)}(\boldsymbol{P}^{*(\tau-1)})) \leq C_l(\boldsymbol{P}^{*(\tau)}) \tag{45}$$

where the above inequality comes from (42). By using Theorem 1, we also have

$$C_l(\boldsymbol{P}^{*(\tau)}) = \tilde{C}_l(\boldsymbol{P}^{*(\tau)}, \boldsymbol{w}^{l,(\tau+1)}(\boldsymbol{P}^{*(\tau)})) \tag{46}$$

If $\lim_{\tau\to\infty} \|\boldsymbol{P}^{*(\tau)} - \boldsymbol{P}^{*(\tau-1)}\| = 0$, then $\tilde{C}_l(\boldsymbol{P}^{*(\tau)}, \boldsymbol{w}^{l,(\tau)}(\boldsymbol{P}^{*(\tau-1)})) = \tilde{C}_l(\boldsymbol{P}^{*(\tau)}, \boldsymbol{w}^{l,(\tau+1)}(\boldsymbol{P}^{*(\tau)}))$ is a consequence of the tightening steps. At this time, the ingress rate and egress rate of each link in networks are optimally balanced at $(\boldsymbol{x}^{*(\tau)}, \boldsymbol{P}^{*(\tau)})$

$$\sum_{s\in S(l)} x_s^{*(\tau)} = \tilde{C}_l(\boldsymbol{P}^{*(\tau)}, \boldsymbol{w}^{l,(\tau+1)}(\boldsymbol{P}^{*(\tau)})) = C_l(\boldsymbol{P}^{*(\tau)}) \tag{47}$$

13 Appendix 5: Proof of Theorem 3

Propositions 3–5 show that the solutions of this series of approximations converge to a stationary point satisfying the necessary optimality KKT conditions of the original problem $\boldsymbol{P}1$. From (47), the complementary slackness is zero and our link capacity approximation becomes exact, that is, link capacity constraints in (6) are active. In other words, PU outage constraint is always active at each iteration τth. Hence, it will be active if $\lim_{\tau\to\infty} \|\boldsymbol{P}^{*(\tau)} - \boldsymbol{P}^{*(\tau-1)}\| = 0$. Furthermore, the utility function is assumed to be concave $\forall \boldsymbol{x} \in \mathcal{X}$, it then follows that $(\boldsymbol{x}^{*(\tau)}, \boldsymbol{P}^{*(\tau)})$ is a global optimum of the original problem $\boldsymbol{P}1$.

14 Appendix 6: Proof of Proposition 5

SIR constraints (34) show that $I_{-l}(\boldsymbol{P})$ is a function which satisfies the triple properties of positivity, monotonicity, and scalability for all $\boldsymbol{P} \in \mathcal{P}$. Since $\nu(\rho_l P_l/1 + \rho_l P_l) \geq 0$, we have

$$P_l^{(t)} \geq I_{-l}(\boldsymbol{P}^{(t)}) \geq I_{-l}(\boldsymbol{P}^{(t)}) - \nu^{(t)}\frac{\rho_l P_l^{(t)}}{1+\rho_l P_l^{(t)}} = P_l^{(t+1)}, \quad \forall l \in \mathcal{L}$$

Hence, $P_l^{(t)}$ is a monotonic decreasing sequence. This sequence has the lower bound of $P_l^{\min}$, the power control algorithm always converges to the a unique limit point $P_l^{(*)}$.

doi: 10.1049/iet-net.2011.0028

15 Appendix 7: Proof of Theorem 4

Since the PU outage price $\nu^{(t)} \to \nu^*$ almost surely when $T \to \infty$ and $T \to \infty$ [13]. Furthermore, in the iterative procedure of Sop-JRPC, the congestion control part is referred as the current step whereas the power control part stems from the solution of the previous step. In each step, only the former which is convex is maximised and the obtained solution is used for forming a new convex approximation (33) of the non-convex power allocation subproblem of (30). The results achieved from this new convex problem are used for the next iteration of algorithm. Hence the optimal solution of Sop-JRPC may be considered a sub-optimal solution of the original problem $\boldsymbol{P}1$.

doi: 10.1049/iet-net.2011.0028